Modeling physical systems by effective harmonic oscillators: The optimized quadratic approximation

Jianshu Cao and Gregory A. Voth
Department of Chemistry, University of Pennsylvania, Philadelphia, Pennsylvania 19104-6323

(Received 18 August 1994; accepted 8 November 1994)

A mathematical formalism is developed to map a physical system described by a general potential energy function onto one consisting of effective harmonic oscillators. The present focus is on many-body systems characterized by a temperature, so the theoretical effort is devoted to the partition function through a diagrammatic representation of its cumulant expansion in the quadratic reference system. Appropriate diagram summation and renormalization strategies lead to an ''optimized quadratic approximation'' (OQA) for both the quantum and classical partition functions of general systems. Diagrammatic methods are also used to develop accurate higher order corrections to the OQA. Applications to representative problems are presented with good success. © *1995 American Institute of Physics.*

I. INTRODUCTION

Many challenges faced by the theorist have a single origin: Virtually all nontrivial physical problems cannot be solved exactly with known mathematical techniques. Yet, this situation also gives rise to many stimulating opportunities for one to develop *approximate* techniques to analyze such problems. For example, computational approaches have grown enormously in popularity within this context, yielding important new insights into the behavior of complex physical systems. Another fruitful approach has been to model complex systems by simpler ''zeroth-order'' systems which *can* be analyzed exactly, and to then use perturbation theory to quantify that which is missing from the zeroth-order description. Yet another strategy is to map the solution of a difficult problem onto one which is easier to understand mathematically. This latter approach falls within the domain of *variational theory*, out of which has grown such important techniques as self-consistent and mean field methods, basis set expansions, density functional methods, wave packet dynamics, effective potential theories, etc. One drawback of the variational method, however, is that it can often be unclear how to judge the accuracy of the variational solution and then to systematically *improve upon* that solution. The focus of the present paper, therefore, is devoted to the latter issue within the context of one particular variational theory. In particular, the technique of representing a general nonlinear potential energy function by an effective harmonic function (see, e.g., Ref. 1) will be formally analyzed within the context of statistical mechanics, and then it will be shown how to systematically improve upon the variational solution to this problem.

In an earlier study,[2] a theory was developed for the equilibrium path centroid density in the Feynman path integral representation of quantum statistical mechanics.[1,3–9] In that work, the Feynman path *fluctuations* about the centroid variable were expressed in terms of a quadratic reference action functional. A one-to-one correspondence was developed between a diagrammatic representation and the cumulant expansion of the centroid density in this reference system. It was shown that diagrammatic topological reduction and summation techniques, along with a renormalization of the two basic diagram elements, leads to a set of highly accurate self-consistent equations for the centroid density and related quantities. This analytical theory[2] explores the specific diagrammatic representation of the well-known Feynman–Hibbs variational theory[10] for the centroid density and a more accurate effective quadratic approximation,[11–13] thereby providing a systematic way to improve upon those schemes (see also Ref. 14).

Mathematically, the treatment in Ref. 2 is simply a generalized theory of Gaussian expansions with special care exercised to enforce the centroid constraint. Though the diagrammatic analysis in that paper was developed in the context of the centroid density, the basic methodology is by no means limited to treating only quantum thermal fluctuations around the path centroid. In fact, the only assumption for the validity of this diagrammatic analysis is the quadratic nature of the reference system. In the present paper, therefore, the perspective is significantly broadened to develop a general quadratic reference theory for the *partition function* in both quantum and classical equilibrium statistical mechanics. The theory approximates the physical *potential* as being described by an effective quadratic function, not just the part describing the contribution to the action from the Feynman path fluctuations.

It is well known that any analytic function of Gaussian variables can be uniquely expressed in terms of its first and second moments. In particular, the partition function can be expanded in an arbitrary quadratic reference frame, and the topological reduction of the diagrammatic representation of this expansion leads to a cumulant expansion. Unlike the similar expansion of the centroid density where the centroid of the path fluctuations is constrained,[2] the expression for the partition function includes both the first and second moments so that additional effort is required in the summation and renormalization scheme. Such a procedure treats the classical and quantum thermal fluctuations in a most general fashion, leading to something we term the ''optimized quadratic approximation'' (OQA) and higher order corrections. At ex-

 0021-9606/95/102(8)/3337/12/$6.00

tremely low temperatures, the OQA and higher order corrections can be shown to be equivalent to a quantum perturbation theory calculation. At high temperatures, the OQA approximation does not recover the exact classical limit as does the centroid theory. Indeed, in the classical OQA the potential is still modeled by an optimized quadratic function.

The formal OQA theory is presented in Sec II, with some aspects of the diagrammatic analysis having been already elaborated in Ref. 2 to which the reader is referred for more details. In Sec. III, applications of the OQA theory are presented. Specifically, in order to demonstrate the validity and utility of the OQA scheme and higher order corrections, the classical and quantum partition functions for a particle in a one dimensional anharmonic potential are calculated at several temperatures. The comparison with the exact results obtained by path integral Monte Carlo simulations[9] clearly indicates a consistent improvement as the higher levels of corrections are included. Next, the nonlinear dipolar interaction in fluids is formulated in the context of the OQA equations. Combination of this formalism and the mean field approximation (MSA)[15–19] provides a means to study the dielectric response of polarizable fluids including nonlinear dipolar interactions. To probe the extremely quantum mechanical limit of the theory, the ground state energy shift of a Drude oscillator in the presence of an electron[20] is calculated. The results are compared with the exact data computed via path integral Monte Carlo simulations. Finally, the analytic continuation of imaginary time correlation functions generated from the OQA theory is employed to study intramolecular vibrational relaxation in polyatomic molecules, demonstrating a connection to some expressions derived by others.[21] Concluding remarks are given in Sec IV.

II. THEORY

A. Exact diagrammatic representation of the partition function

For the sake of simplicity, the OQA theory will be developed in this section for a one-dimensional quantum particle. From this analysis, the generalization to multidimensional space is straightforward. The classical limit may be recovered by taking Planck's constant $\hbar$ to zero.

Two basic elements are required to specify a general quadratic reference potential: (1) the average position in the reference system, given by

$$\bar{q}_r = \langle q \rangle_{\rm ref} \tag{2.1}$$

and (2) the imaginary time correlation function in the reference system, given by

$$\alpha(\tau) = \langle (q(\tau) - \bar{q}_r)(q(0) - \bar{q}_r) \rangle_{\rm ref}, \tag{2.2}$$

where τ is the imaginary time on the interval $0 \leqslant \tau \leqslant \hbar\beta$. It is well known that any function of a Gaussian variable can be expressed in terms of its mean $\bar{q}_r$ and its mean squared deviation $\alpha(\tau)$. All average values in the quadratic reference potential are denoted by the symbol $\langle \cdots \rangle_{\rm ref}$.

Since the correlation function in Eq. (2.2) is defined with respect to the reference mean, an arbitrary Feynman path can be decomposed as $q(\tau) = \bar{q}_r + \tilde{q}(\tau)$, where $\tilde{q}(\tau)$ is the thermal fluctuation about the reference mean. A Fourier decomposition of the fluctuation paths $\tilde{q}(\tau)$ can now be introduced such that

$$\tilde{q}(\tau) = \sum_{n=-\infty}^{\infty} \hat{q}_n e^{-i\Omega_n \tau}, \tag{2.3}$$

where the summation is over all integers, and Ω_n is the Matsubara frequency defined by $\Omega_n = 2\pi n/\hbar\beta$. (It should be noted that the above path decomposition is different from that in Ref. 2 where the path fluctuations about the centroid variable where studied.) As a next step, the imaginary time action in the quadratic reference system is specified to have a quadratic form in the variable $\tilde{q}(\tau)$ such that

$$S_{\rm ref}[\tilde{q}(\tau)]/\hbar = \frac{1}{\hbar} \sum_{0}^{\hbar\beta} d\tau \left\{ \frac{m}{2} \dot{\tilde{q}}(\tau)^2 + V_{\rm ref}[\tilde{q}(\tau)] \right\}$$

$$= \sum_{n=-\infty}^{\infty} \frac{|\hat{q}_n|^2}{2\alpha_n}, \tag{2.4}$$

where α_n defines the reference correlation function such that

$$\alpha(\tau) = \sum_{n=-\infty}^{\infty} \alpha_n e^{-i\Omega_n \tau}. \tag{2.5}$$

To be specific, for the effective quadratic reference potential, given by $V_{\rm ref}(q) = (1/2) m\omega^2 (q - \bar{q}_r)^2$, one has according to Eq. (2.4)

$$\alpha_n = \frac{1}{m\beta(\Omega_n^2 + \omega^2)} \tag{2.6}$$

which leads to the imaginary time correlation function

$$\alpha(\tau) = \frac{\hbar}{2m\omega} \frac{\cosh[(1-2u)b/2]}{\sinh(b/2)}, \tag{2.7}$$

where $b = \hbar\beta\omega$ and $u = \tau/\hbar\beta$. In the classical limit, $\alpha(\tau)$ reduces to the constant $\alpha = 1/(m\omega^2\beta)$ and all α_n vanish except for α_0.

In terms of the quadratic reference system introduced above, one can express the partition function as

$$Z = Z_{\rm ref} \langle \exp(-\beta \overline{\Delta V}) \rangle_{\rm ref}, \tag{2.8}$$

where $\overline{\Delta V}$ is the imaginary time average

$$\overline{\Delta V} = \frac{1}{\hbar\beta} \int_0^{\hbar\beta} d\tau \, \Delta V(q(\tau)), \tag{2.9}$$

and $\Delta V \equiv V - V_{\rm ref}$ is the deviation of the real potential V from the reference potential $V_{\rm ref}$.

In order to develop a diagrammatic theory for the partition function, one must first Taylor expand the average in Eq. (2.8), giving

$$\langle \exp(-\beta\overline{\Delta V})\rangle_{\mathrm{ref}} = \sum_{n=0}^{\infty} \frac{1}{n!} \left\langle \left[-\frac{1}{\hbar} \int_0^{\hbar\beta} d\tau\, \Delta V(q(\tau)) \right]^n \right\rangle_{\mathrm{ref}} , = \sum_{n=0}^{\infty} \frac{1}{n!} \left\langle \left[-\frac{1}{\hbar} \int_0^{\hbar\beta} d\tau \int \frac{dk}{2\pi}\, \Delta\hat{V}(k) e^{ikq(\tau)} \right]^n \right\rangle_{\mathrm{ref}} , \tag{2.10}$$

where $\Delta\hat{V}(k)$ is the spatial Fourier transform of the potential difference $\Delta V(q)$ with respect to the variable q. Since $q(\tau_i)$ is a Gaussian variable in the reference system at any imaginary time slice τ_i, the cumulant expansion of a linear combination of those variables truncates at second order, giving

$$\left\langle \prod_{i=1}^{n} e^{ik_i q(\tau_i)} \right\rangle_{\mathrm{ref}} = \exp\left\{ -\left[i\sum_{i=1}^{n} k_i \bar{q}_r + \frac{1}{2} \sum_{i=1}^{n} \sum_{j=1}^{n} k_i k_j \alpha(\tau_i - \tau_j) \right] \right\} \tag{2.11}$$

in which the mean and the Gaussian width are given in Eq. (2.1) and Eq. (2.2), respectively. It is noted that in a similar expansion[2] for the centroid density there exist no terms linear in k_i or terms containing α_0 according to the definition of the centroid variable. This difference leads to additional factors in Eq. (2.11) which do no appear in the theory for the centroid density.

By substituting the Taylor expansion of Eq. (2.11) into Eq. (2.10), and transforming back into coordinate space, one arrives at the final expression in terms of the mean coordinate, the Gaussian width, the partial derivatives of potential, and integrations over the imaginary time τ. It is not particularly useful to explicitly write out this lengthy expression here even though the perturbation series gives, in principle, a complete description of the quantum canonical ensemble. Instead, a set of diagrammatic symbols will be introduced to aid in specifying the pertinent analytical expressions. It is likely that in higher orders the expansion terms become increasingly complicated and a low order calculation will not provide a reasonable physics picture of a quantum system having large anharmonicities. A suitably devised diagrammatic representation, therefore, is not only a useful tool to keep track of the expansion terms but also a powerful way to analyze the perturbation series. This is no different from a host of other applications of diagrammatic methods in physical science (see, e.g., Refs. 22 and 23).

There are three basic elements composing the diagrams in the expansion of Eq. (2.8): vertices, dashed lines, and solid lines. Each vertex is associated with the potential, or its derivatives and an imaginary time τ_i to be integrated from $\tau_i=0$ to $\tau_i=\hbar\beta$. The potential terms are to be evaluated at the origin of coordinate space. Each dashed line with only one end attached to a vertex and the other end free (an open line) is designated as the reference mean value $\bar{q}_r$. Each solid line connecting two vertices at times τ_i and τ_j denotes a reference correlation function $\alpha(\tau_i-\tau_j)$. Whenever a line connects to a vertex, a spatial derivative is applied to the potential so that the order of the derivative is equal to the number of lines that connect to the vertex. A negative sign and a factor of $1/\hbar$ are assigned to each vertex. The value of a diagram is the product of all the composing elements multiplied by a symmetry coefficient determined by the topological structure of the diagram.

With the above definitions, a one-to-one correspondence can be established between each distinct perturbation term and each diagram. The expansion series in Eq. (2.10) is then the collection of all topologically different diagrams and all possible combinations. It is well known that an infinite series of all possible topologically different diagrams, and their combinations, is equal to the exponential of all possible topologically different connected diagrams.[22] For a connected diagram, any two parts of the diagram are linked to each other by at least one line, one vertex, or one path of lines. Therefore, one can express the quantum partition function as

$$Z = Z_{\mathrm{ref}} \exp(\mathscr{F}), \tag{2.12}$$

where $\mathscr{F}$ is given by

$\mathscr{F}=$ 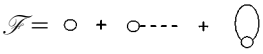 . (2.13)

Though the topological reduction performed in the present case is equivalent to a diagrammatic representation of the cumulant expansion, the cumulant expansion itself becomes complex in higher orders and there are a large number of cancellations not explicitly obvious in the cumulant relations. It therefore proves to be much easier to keep track of higher order terms using the diagrammatic representation.

To illustrate the usage of the diagrammatic expansion, two simple identities must first be established, i.e.,

$-\beta\Delta V(\bar{q}_r)=$ 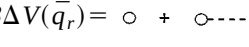 , (2.14)

which evaluates the potential at position $\bar{q}_r$, and

$-\beta\langle \Delta V(\tilde{q})\rangle_{\alpha}=$ 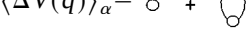 , (2.15)

which yields a Gaussian averaged potential at the origin, the Gaussian width being given by

$$\alpha(0) = \frac{\hbar}{2m\omega} \coth(b/2). \tag{2.16}$$

Combination of the above two expressions leads to the average potential in the reference system, giving

$$-\beta\langle \Delta V\rangle_{\rm ref} =$$ 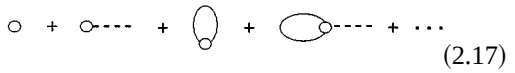 (2.17)

which consists of all topologically different decorations derived from the diagrams in Eq. (2.14) and Eq. (2.15). Since the mean and the width of the reference quadratic potential uniquely define an infinite set of Gaussian variables $\{\hat{q}_n\}$, one can equivalently denote the average in the reference system as

$$\langle \Delta V\rangle_{\rm ref} = \langle \Delta V(\bar{q}_r+\tilde{q})\rangle_\alpha = \frac{1}{\sqrt{2\pi\alpha(0)}} \int d\tilde{q}\ \Delta V(\bar{q}_r + \tilde{q}) \exp[-\tilde{q}^2/2\alpha(0)], \tag{2.18}$$

where the Gaussian width is defined in Eq. (2.16). The simple diagram series in Eq. (2.17) then yields the leading approximation to the partition function, i.e.,

$$Z \simeq Z_{\rm ref}\ \exp(-\beta\langle \Delta V\rangle_{\rm ref}), \tag{2.19}$$

which sets an upper bound to the true partition function.[1] An application of the Gibbs–Bogoliubov variational principle to Eq. (2.19) will lead to an optimized quadratic reference potential which will be derived from a different point of view in the next subsection.

B. Optimized quadratic approximation

As has been demonstrated in the previous work on the centroid density,[2] a similar expression for $\mathscr{F}$ in the centroid density expansion consists of closed diagrams, i.e., there exists no class of diagrams in $\mathscr{F}$ with single lines hanging outside the main diagram or connecting two separate parts of diagrams. Therefore, the expression for $\mathscr{F}$ in Eq. (2.13) represents a larger set of diagrams than in the centroid theory and additional renormalization schemes must be introduced to simplify the summation of diagrams. This procedure leads to equations for the average position and the self-consistent frequency, thus resulting in the general optimized quadratic approximation. In the context of the diagrammatic theory developed in Ref. 2, the present study is devoted to the consequences of including in the theory an additional set of diagrams having single connected lines.

To address the effects due to the presence of the dashed lines, the average position $\langle q\rangle$ is first introduced through the differentiation of a generating functional. An imaginary time-independent force $f(\tau)$ is introduced into the action functional by replacing $V[q(\tau)]$ with $V[q(\tau)]+f(\tau)q(\tau)$. The average position is then given by

$$\langle q\rangle = \lim_{f\to 0} -\hbar\ \frac{\delta \ln Z[f]}{\delta f(0)} \tag{2.20}$$

where $Z[f]$ is the corresponding partition function for the potential $V+fq$.

Clearly the linear force term fq adds to the diagrams for $\mathscr{F}$ in Eq. (2.13) a solid or dashed line with one end associated with f, giving

$$\langle q\rangle =$$ (2.21)

Making use of the identity in Eq. (2.17), one can renormalize a major portion of the above infinite series by defining

$$\bar{q} =$$ (2.22)

or in an explicit analytical form as

$$\bar{q} = \bar{q}_r - \beta\alpha_0\langle \Delta V^{(1)}(\bar{q}+\tilde{q})\rangle_\alpha . \tag{2.23}$$

Hereafter, quantities with bars stand for renormalized quantities which are represented in the diagrams by bold lines or black vertices. Unlike the centroid density where the mean of the Gaussian average is fixed, the additional subset of diagrams in Eq. (2.13) leads to a self-consistent equation which determines the optimized average position.

To renormalize the lines, one can adopt the chain collection of Eq. (3.35) of Ref. 2, which leads to the following self-consistent equation:

$$\bar{\alpha}(\tau) = \alpha(\tau) - \beta\Delta\bar{V}^{(2)}\ \frac{1}{\hbar\beta}\int_0^{\hbar\beta} d\tau'\ \bar{\alpha}(\tau-\tau')\alpha(\tau'). \tag{2.24}$$

The open line equation in Eq. (2.23) can be rewritten as

$$\bar{q} = \bar{q}_r - \beta\alpha_0\Delta\bar{V}^{(1)} \tag{2.25}$$

which is to be solved simultaneously with the bold line renormalization equation in Eq. (2.24). Here, the average potential or its derivative is fully renormalized and is given by

$$\Delta\bar{V}^{(n)} = \langle \Delta V^{(n)}(\bar{q}+\tilde{q})\rangle_{\bar{\alpha}} \tag{2.26}$$

which implies that each black vertex is attached with all possible decorations of single line diagrams, the loops and rings.

There is a simple solution to Eqs. (2.24)–(2.25) if the following conditions are satisfied:

$$\langle \Delta V^{(1)}(\bar{q}+\tilde{q})\rangle_{\bar{\alpha}} = 0, \tag{2.27}$$

$$\langle \Delta V^{(2)}(\bar{q}+\tilde{q})\rangle_{\bar{\alpha}} = 0, \tag{2.28}$$

which leads to $\bar{q}=\bar{q}_r$ and $\bar{\alpha}=\alpha(0)$. One can thus introduce the optimized quadratic approximation (OQA), where the reference potential takes the form of

$$V_{\rm OQA} = \tfrac{1}{2}m\bar{\omega}^2(q-\bar{q})^2 \tag{2.29}$$

with the parameters $\bar{\omega}$ and $\bar{q}$ implicitly defined by Eqs. (2.27)–(2.28). The OQA potential of Eq. (2.29) represents the best quadratic fit to an anharmonic potential. If the average is constrained at a fixed position as in the case of the centroid density, all the results in Ref. 2 can be recovered. Unlike the centroid theory which is exact in the classical limit, the OQA theory and higher order corrections forms an approximate representation of classical systems. The validity of the theory in either case depends on the anharmonicity of

the potential and the temperature of the system. At low temperatures, quantum thermal fluctuations play a major role; at higher temperatures, the system is more likely to experience nonlinear regions of large anharmonicities. The present theory incorporates these effects in a self-consistent fashion, manifested by the interplay between the average position $\bar{q}$ and the effective frequency $\bar{\omega}$.

As in the formulation of the locally optimized quadratic approximation to the centroid density[2,11–13] and the centroid-constrained propagator,[2] the OQA equations can also be obtained by applying the Gibbs–Bogoliubov variational procedure to maximize the right-hand side of Eq. (2.19) with respect to the parameters $\bar{\omega}$ and $\bar{q}$, leading to Eqs. (2.27) and (2.28). On the other hand, the diagrammatic representation provides a systematic study of the formally exact perturbation series, reveals the relationship between the variational method and the renormalization of the perturbations terms and, more importantly, makes it possible to *improve upon* the variational OQA approach by including higher order diagrammatic corrections.

For complicated potential surfaces, and especially for many-body systems, there are many possible solutions to OQA equations. Physically all of these solutions correspond to metastable potential wells. Under the condition that the wells are reasonably separated, i.e., the barrier between any two neighboring wells is significantly higher than the average thermal energy, one can assume the partition function is given by a linear superposition for all the metastable solutions. In this spirit, the partition function in the OQA can be written as

$$Z=\sum_l Z_l \exp(-\beta\Delta\bar{V}_l), \tag{2.30}$$

where $\{l\}$ denotes the set of distinct solutions to Eqs. (2.27)–(2.28). In general, all expectation values evaluated in the OQA theory would follow this superposition principle.

In a way, one can attribute the differences between liquids and solids to the nature of the OQA solutions for the many-body configurations. Indeed, this important concept makes it possible to define for liquids inherent structures, which were previously proposed and pursued from the perspective of quenched potential minima,[24–27] and to make a connection with the somewhat different concept of instantaneous normal modes (INM),[28–31] which provide an extension of the phonon picture of solids.[32,33] However, the unstable modes in the INM theory present a conceptual difficulty when formulating the INM expression for dynamical correlation functions (i.e., they must be thrown out or the INM expression will unphysically diverge at long times). The inherent normal modes, defined as solutions to the OQA equations, are free of such unstable modes by definition, and thus appear to provide a more accurate description of liquid state dynamical correlations. Progress on this latter aspect of the theory will be presented in a forthcoming paper.[34]

C. Higher order corrections to the partition function

In principle, the perturbation series does not depend on a specific effective quadratic reference potential because when one includes a sufficient number of terms the series will yield the desired accuracy. Nevertheless, a good choice of the reference potential will give improved convergence and simplify the diagrammatic analysis; in particular, the OQA reference potential will bear the closest resemblance to the real potential. The OQA conditions specify that all vertices linked to one line or two lines will vanish, i.e.,

$$= 0 \tag{2.31}$$

$$= 0 \tag{2.32}$$

where the lines can be either solid or dashed. Furthermore, if one chooses the origin at $\bar{q}$ and redefines the coordinate according to $\tilde{q}=q-\bar{q}$, all the dashed lines will vanish. Consequently, imposing the optimization equations eliminates a large number of diagrams containing the above two elements.

Since all diagrams containing the above elements will vanish, the leading corrections in $\mathscr{F}$ in Eq. (2.13) are then given by


$$= \frac{1}{2!3!}\frac{\beta}{\hbar}\int_0^{\hbar\beta} d\tau\, \bar{\alpha}^3(\tau)(\Delta\bar{V}^{(3)})^2 \tag{2.33}$$

and


$$= \frac{1}{2!4!}\frac{\beta}{\hbar}\int_0^{\hbar\beta} d\tau\, \bar{\alpha}^4(\tau)(\Delta\bar{V}^{(4)})^2 \tag{2.34}$$

where all quantities are evaluated in the OQA reference system. The above two terms provide an improvement to the OQA partition function, giving

$$Z=Z_{\mathrm{OQA}}\exp\left\{-\beta\left[\Delta\bar{V}-\frac{1}{2!3!}\frac{f_3(b)}{\hbar\bar{\omega}}\left(\frac{\hbar}{m\bar{\omega}}\right)^3(\Delta\bar{V}^{(3)})^2 - \frac{1}{2!4!}\frac{f_4(b)}{\hbar\bar{\omega}}\left(\frac{\hbar}{m\bar{\omega}}\right)^4(\Delta\bar{V}^{(4)})^2+\cdots\right]\right\}, \tag{2.35}$$

where $b=\hbar\bar{\omega}\beta$. Here, $f_n(b)$ is a dimensionless coefficient, defined by

$$f_n(b)=\left(\frac{1}{b}\right)^{n-1}\int_0^1 du\left[\frac{b/2}{\sinh(b/2)}\cosh(1-2u)b/2\right]^n \tag{2.36}$$

which becomes a constant in the large b limit. More corrections can be included by adding more diagrams.

At extremely low temperatures, the quantum partition function is dominated by the contribution from the ground state, i.e.,

$$E_0=\lim_{\beta\to\infty}\frac{1}{\beta}\ln Z(\beta). \tag{2.37}$$

It is therefore an important test to calculate the ground state energy from the OQA theory. This procedure can be shown to be equivalent to the quantum perturbation theory expression based on a basis set consisting of LHO (linear harmonic oscillator) eigenstates. As an example, consider the cubic oscillator potential, given by

$$V(q)=\tfrac{1}{2}m\omega^2q^2+cq^3. \tag{2.38}$$

The reference potential is simply the LHO term, i.e., $V_{\rm ref}=(1/2)m\omega^2q^2$. Though the reference potential is not optimized, a single vertex and all the vertices linked to one line or two lines will vanish. Therefore, the leading correction terms to the partition function are given as

$\mathcal{F}=$  , (2.39)

which then leads to the expression for the ground state energy

$$E_0=\frac{1}{2}\hbar\omega-9\,\frac{c^2}{\hbar\omega}\lambda^6-2\,\frac{c^2}{\hbar\omega}\lambda^6+\cdots . \tag{2.40}$$

Here, the following relations in the low temperature limit are used

$$\lim_{\beta\to\infty} f_n(b)=\frac{1}{2^{(n-1)}n} \tag{2.41}$$

and

$$\lim_{\beta\to\infty}\alpha(0)=\frac{\hbar}{2\omega m}=\lambda^2, \tag{2.42}$$

with λ being the width of the ground state LHO wave function. It can be readily verified that the first correction corresponding to the first diagram in Eq. (2.39) is identical to the second order perturbation expression due to the coupling between the zeroth and the third LHO eigenvector, and the second correction corresponding to the second diagram in Eq. (2.39) is identical to the second order perturbation expression due to the coupling between the zeroth and the first LHO eigenvector. Evidently, a one-to-one correspondence can be established between perturbation terms of the ground state energy calculation and higher order diagrams evaluated in the low temperature quantum mechanical limit. In the next section, this method will be applied to calculate the ground state energy of a Drude oscillator interacting with an electron.

It has been a common practice in ground state calculations to first variationally parameterize the wave function from a reference potential and then the perturbation solution is introduced to improve on the accuracy.[35] We note that the the general quadratic theory presented here is analogous to this approach, but it is extended through the incorporation of thermal excitations. Moreover, as long as the potential is a regular function, one can in principle include more diagrams into the calculations to achieve higher accuracy.

D. Higher order corrections to the correlation function

The imaginary time position correlation function $C(\tau)$ can be introduced through functional differentiation of a generating functional. In order to formulate such a functional, an imaginary time-dependent force $f(\tau)$ is introduced into the action functional of the partition function such that the potential $V[q(\tau)]$ is replaced by $V[q(\tau)]+f(\tau)\tilde{q}(\tau)$. The correlation function is thus given by

$$\langle q(\tau)q(0)\rangle=\lim_{f\to 0}\frac{\hbar^2}{Z}\frac{\delta^2 Z[f(\tau)]}{\delta f(\tau)\delta f(0)}. \tag{2.43}$$

Here, the partition function $Z[f(\tau)]$ is understood to be a functional of the extra time-dependent force $f(\tau)$ and is therefore the generating functional for the imaginary time correlation function.

Following the diagrammatic notation introduced in the previous subsections, one can formally express the correlation function as:

$\langle q(\tau)q(0)\rangle=$ 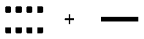 , (2.44)

where the bold solid line stands for the collection of all the possible connected diagrams linking two ends associated with $f(\tau)$ and $f(0)$, and the bold dashed line stands for the average position. To simplify the analysis, we redefine the position correlation function as

$$C(\tau)=\langle(q(\tau)-\langle q\rangle)(q(0)-\langle q\rangle)\rangle \tag{2.45}$$

in which the average position $\langle q\rangle$ can be the exact result evaluated from simulations or the analytical solution calculated from the renormalization equation Eq. (2.25). With this definition in hand, the evaluation of the correlation function $C(\tau)$ is equivalent to the renormalization of the solid line [i.e., the bold solid line in Eq. (2.44)], explicitly given by Eq. (3.33) in Ref. 2. Here, as stated earlier, all the decorations attached to the intermediate vertices can be removed if the vertex is renormalized. This operation is achieved by replacing all the ΔV's by $\Delta\bar{V}$'s, giving

$$\Delta\bar{V}=\langle\Delta V(\langle q\rangle+\tilde{q})\rangle_{C(0)} \tag{2.46}$$

where the Gaussian width is now denoted by $C(0)$ instead of $\alpha(0)$. In the case of full renormalization, $C(\tau)$ is equivalent to the renormalized reference correlation function $\bar{\alpha}(\tau)$, and $\langle q\rangle$ is equivalent to the renormalized reference mean $\bar{q}$. These two notations will not be distinguished hereafter.

The simplest set of lines, given by Eq. (3.35) of Ref. 2, is the chain collection, which leads to the following self-consistent equation:

$$\bar{\alpha}_n=\alpha_n-\beta\Delta\bar{V}^{(2)}\bar{\alpha}_n\alpha_n . \tag{2.47}$$

By noting that $\bar{\alpha}=\Sigma\bar{\alpha}_n$, it is seen that Eq. (2.47) is the same as the OQA equation (2.28) derived earlier.

The next stage in the analysis is to include all the two-line-loop corrections in the renormalization, given by Eq. (3.38) of Ref. 2. It is important to incorporate infinite terms corresponding to the same class of diagrams so that at low temperature and high anharmonicity the self-consistent equation will not diverge. The infinite summation of two-line loops in Eq. (3.38) of Ref. 2 can be carried out to yield a closed equation, given by

$$\bar{\alpha}_n=\alpha_n-\alpha_n\bar{\alpha}_n\beta\Delta\bar{V}^{(2)}+\frac{(1/2)\alpha_n\bar{\alpha}_n\overline{\alpha_n^2}(\beta\Delta\bar{V}^{(3)})^2}{1+(1/2)\overline{\alpha_n^2}(\beta\Delta\bar{V}^{(4)})} \tag{2.48}$$

which can be solved numerically. Here, $\overline{\alpha_n^2}$ is the contribution from the two-line-loop diagram, given by

$$\overline{\alpha_n^2} = \sum_{m=-\infty}^{\infty} \bar{\alpha}_{n-m}\bar{\alpha}_m, \tag{2.49}$$

where α_n is interpreted as in Eq. (2.7) which in the classical limit becomes zero unless n is zero. Since $\overline{\alpha^2}$ is a convolution expression, the self-consistent equation for $\bar{\alpha}$ is nonlocal in Fourier space, and therefore one can no longer seek a single effective frequency prescription as in the OQA theory. In fact, this analysis shows that the optimized quadratic reference system provides the best possible quadratic potential to approximate an anharmonic potential and any further corrections are beyond the effective quadratic description.

The real-time counterpart of the imaginary time quantum correlation function $C(\tau)$ is an essential component in describing the dynamics of quantum systems. The real time and imaginary time correlation functions are of course related by the analytical continuation $\tau \rightarrow it$, so the detailed study of the Euclidean correlation function presented in this section may eventually help to reveal the real time behavior of quantum systems.[36,37] As an example, it will be demonstrated in Sec. III D that Eq. (2.48) can be employed in studying intramolecular vibrational relaxation in polyatomic molecules.

E. Multidimensional formulation

In order to generalize the OQA theory to multidimensional coordinate space, a vector-matrix prescription will be introduced here to formalize the relevant expressions. Here, vectors and matrices are denoted by bold fonts.

First, the OQA equations [Eqs. (2.27)–(2.28)] can be rewritten as

$$\langle \boldsymbol{\nabla} V(\bar{\mathbf{q}}+\tilde{\mathbf{q}})\rangle_{\mathbf{C}} = 0 \tag{2.50}$$

$$\langle \boldsymbol{\nabla}:\boldsymbol{\nabla} V(\bar{\mathbf{q}}+\tilde{\mathbf{q}})\rangle_{\mathbf{C}} = \mathbf{K}, \tag{2.51}$$

where $\mathbf{K}$ is the optimized effective force constant matrix and where $\boldsymbol{\nabla}$ is the partial derivative vector with the elements $\boldsymbol{\nabla}_i = \partial_i$. The notation $\langle \cdots \rangle_{\mathbf{C}}$ here denotes a multidimensional Gaussian average centered at $\bar{\mathbf{q}}$, i.e.,

$$\langle V(\bar{\mathbf{q}}+\tilde{\mathbf{q}})\rangle_{\mathbf{C}} = \frac{1}{\sqrt{\det[2\pi\mathbf{C}]}} \int d\tilde{\mathbf{q}}\; V(\bar{\mathbf{q}}+\tilde{\mathbf{q}}) \times \exp(-\tilde{\mathbf{q}}\cdot\mathbf{C}^{-1}\cdot\tilde{\mathbf{q}}/2) \tag{2.52}$$

where the Gaussian width factor matrix $\mathbf{C}$, in this case, can be formally expressed as

$$\mathbf{C} = \sum_{n=-\infty}^{\infty} [\beta\mathbf{m}\Omega_n^2 + \beta\mathbf{K}]^{-1}. \tag{2.53}$$

Here, $\mathbf{m}$ is the N-dimensional mass matrix and $\Omega_n = 2\pi n/\hbar\beta$. In terms of eigensolutions, a unitary matrix $\mathbf{U}$ can be found which diagonalizes the mass-scaled force constant matrix $\mathbf{K}$, giving the eigenfrequencies

$$\mathbf{U}^{\dagger}\bar{\mathbf{K}}\mathbf{U} = [\mathbf{I}\cdot\bar{\omega}^2], \tag{2.54}$$

where $\bar{\omega}$ is the set of the eigenfrequencies and $[\mathbf{I}\cdot\bar{\omega}^2]$ denotes a diagonal matrix with the lth diagonal element given by $\bar{\omega}_l^2$. The Gaussian width factor matrix in Eq. (2.52) can be determined from the relation

$$\mathbf{C} = \bar{\mathbf{U}}[\mathbf{I}\cdot\bar{\alpha}]\bar{\mathbf{U}}^{\dagger}, \tag{2.55}$$

where $\bar{\mathbf{U}} = \mathbf{m}^{-1/2}\mathbf{U}$ and the individual elements of the normal mode thermal width factor vector are related to the normal mode frequencies $\{\omega_l\}$ such that

$$\bar{\alpha}_l = \frac{1}{\beta\bar{\omega}_l^2}\left\{\frac{(\hbar\beta\bar{\omega}_l/2)}{\tanh(\hbar\beta\bar{\omega}_l/2)}\right\}. \tag{2.56}$$

Thus the set of optimized frequencies $\{\bar{\omega}\}$ and average positions $\{\bar{q}\}$ are variationally obtained as the self-consistent solution to the transcendental matrix equations, Eqs. (2.50)–(2.56) in N-dimensional space.

With the help of the vector and matrix notation, one can now rewrite the higher order corrections to the partition function in N-dimensional space as

$$\text{  } = \frac{1}{2!3!}\sum_{\{i,j,k\}}\sum_{\{i',j',k'\}}\frac{\beta}{\hbar} \times \int_0^{\hbar\beta} d\tau\; \mathbf{C}_{ii'}(\tau)\mathbf{C}_{jj'}(\tau) \times \mathbf{C}_{kk'}(\tau)[\partial_i\partial_j\partial_k\Delta\bar{V}][\partial_{i'}\partial_{j'}\partial_{k'}\Delta\bar{V}] \tag{2.57}$$

and

$$\text{  } = \frac{1}{2!4!}\sum_{\{i,j,k,l\}}\sum_{\{i',j',k',l'\}}\frac{\beta}{\hbar} \times \int_0^{\hbar\beta} d\tau\; \mathbf{C}_{ii'}(\tau)\mathbf{C}_{jj'}(\tau)\mathbf{C}_{kk'}(\tau)\mathbf{C}_{ll'}(\tau) \times [\partial_i\partial_j\partial_k\partial_l\Delta\bar{V}][\partial_{i'}\partial_{j'}\partial_{l'}\partial_{k'}\Delta\bar{V}], \tag{2.58}$$

where the sums run from 1 to N. The multidimensional formalism for the renormalization equation of the correlation function, Eq. (2.48), can be expressed in a similar format. More discussion on this aspect of the theory can be found in Sec. III D.

III. APPLICATIONS

A. A one-dimensional example

In this section, a completely nonquadratic model potential is employed to stringently probe the accuracy of the OQA equations and higher order corrections for both the quantum and classical partition functions. The test calculations are based on the potential

$$V(q) = q^3 + q^4/2 \tag{3.1}$$

where the mass m and $\hbar$ are taken to be unity. The inverse temperature β is thus the equivalent to the dimensionless parameter $\beta\hbar\omega$.

First, the optimized quadratic reference potential was found according to the variational equations Eqs. (2.27)–(2.28) which have only one solution for the potential in Eq.

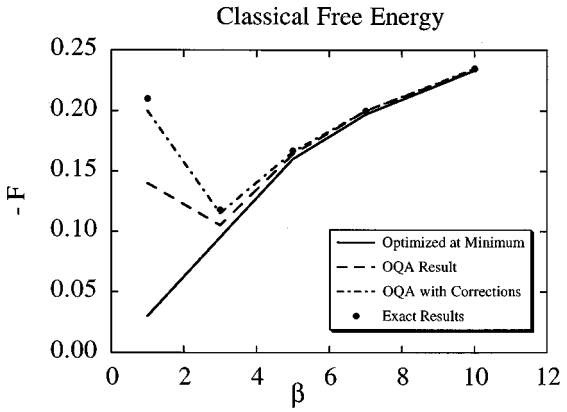

FIG. 1. A plot of the negative free energy, $-F=\ln Z/\beta$, for a classical particle in the potential given by Eq. (3.1). The solid circles depict the numerically exact results, while the solid line is the optimized result of Eq. (2.27) evaluated at potential minimum, the dashed line is the OQA result from Eqs. (2.27)–(2.28), and the dash–dot line is the result obtained by including the higher order correction from Eq. (2.35).

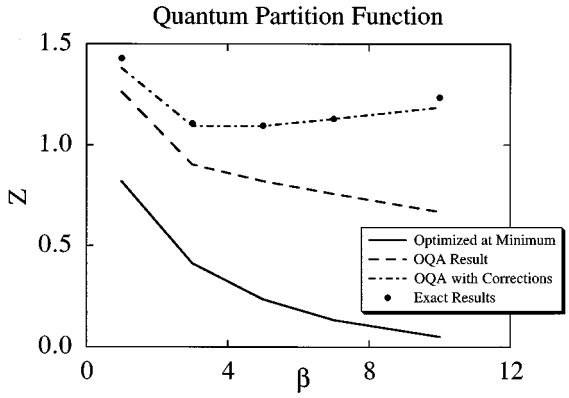

FIG. 2. A plot of the partition function Z for a quantum particle in the potential given by Eq. (3.1). The solid circles depict the numerically exact results, while the solid line is the optimized result of Eq. (2.27) evaluated at potential minimum, the dashed line is the OQA result from Eqs. (2.27)–(2.28), and the dash–dot line is the result obtained by including the higher order correction from Eq. (2.35).

(3.1). The partition function was then evaluated by including the higher order corrections in Eq. (2.35) and compared with the exact result which was obtained by computing the weighting function in Eq. (2.10) directly by Monte Carlo simulations. The umbrella sampling method was employed to evaluate the exact partition function. To achieve good convergence, the path integral simulations[9] employed $P=100$ discretizations and 10^6 MC passes. The number of quasiparticles moved at each trial was adjusted to yield an acceptance ratio of 50%.

In Fig. 1, the magnitude of the negative free energy, $\ln Z/\beta$, for a classical particle in the potential Eq. (3.1) is plotted as a function of β. Without optimizing the equilibrium position through Eq. (2.27), the solution of Eq. (2.28) at the potential minimum deviates considerably from the exact results and the OQA results. This clearly demonstrates the necessity of adjusting the equilibrium position to the center of thermal excitation self-consistently along with the effective thermal fluctuation lengthscale (i.e., the curvature of the effective potential). Furthermore, it is seen in Fig. 1 that the higher order corrections considerably improve upon the OQA solutions. However, all the approximation schemes seem to converge at low temperatures because in this situation a *classical* particle becomes trapped in the potential minimum with diminishing thermal fluctuations.

In Fig. 2, the partition function Z for a quantum particle in the potential of Eq. (3.1) is plotted as a function of β. Again, the progressively improving accuracy of the OQA solutions and the higher order corrections is observed when compared to the results obtained without optimizing the equilibrium position. In this case, however, none of the different approximations completely recover the exact result at low temperature. This error arises because of the nonvanishing quantum ground state amplitude which would require increasingly higher order corrections to describe accurately. The relatively large deviation at higher temperature should also be noted because the increasing thermal fluctuations enable the particle to explore regions of high anharmonicity.

B. Nonlinear effects in dipolar interactions

The rapidly fluctuating motion of electrons (i.e., electronic polarization) has important effects in fluids and clusters (see, e.g., Refs. 38 and 39). A model that incorporates electronic induction is the well studied Drude oscillator model,[15–18,40,41] an isotropic harmonic oscillator with a frequency ω, mass m, and charges $+q$ and $-q$ connected by a harmonic spring. If the electrostatic interaction between the Drude oscillators is treated in the dipole–dipole approximation, the problem reduces to a matrix problem.[19,42,43] This simplified picture of electronic polarization provides a useful vehicle for studying the dielectric and spectral properties of many-body systems.

On the other hand, the dipolar approximation fails to account for the fact that the high order contributions to the Coulomb interaction become important at small distances. To take full account of the Coulomb interactions, one must resort to numerical simulations. However, the variational quadratic reference potential method developed in the present paper allows one to rigorously approximate the Coulomb interactions by a set of general oscillators with coordinates p_i, the effective potential being given by

$$V_{\mathrm{ref}}=\sum_{i=1}^{3N} s_i \frac{p_i^2}{2}+\sum_{i,j=1}^{3N} t_{ij}p_ip_j+\sum_{i=1}^{3N} h_ip_i, \tag{3.2}$$

where N is the number of Drude oscillators and the parameters in the model can be formally defined by the implementation of the general OQA optimization equations, given in this case by

$$s_i=\left\langle \frac{\partial^2 V}{\partial p_i^2}\right\rangle_{\mathrm{C}}, \tag{3.3}$$

$$t_{ij}=\left\langle \frac{\partial^2 V}{\partial p_i \partial p_j} \right\rangle_{\mathbf{C}}, \tag{3.4}$$

$$2h_i=\left\langle \frac{\partial V}{\partial p_i} \right\rangle_{\mathbf{C}}, \tag{3.5}$$

which can be obtained from the application of the optimization conditions in Eqs. (2.50)–(2.51). For every nuclear configuration, the OQA equations specify a set of oscillators which best mimics the Coulomb interacting system, although it could be a formidable numerical task to solve the multidimensional equations.

As an alternative to the direct numerical solution of the OQA equations, the well-developed mean spherical approximation (MSA) for polarizable fluids[15–19] can be combined with the variational approach to yield an optimized MSA equation. The self-consistence is manifested in two different aspects: the many-body polarization and the optimized quadratic approximation.

Consider a pair of Drude oscillators interacting through the Coulombic potential, that is

$$V(\mathbf{R},\mathbf{r}_1,\mathbf{r}_2)=\frac{1}{2}\,m\omega^2\mathbf{r}_1^2+\frac{1}{2}\,m\omega^2\mathbf{r}_2^2+q^2\left[\frac{1}{R}-\frac{1}{|\mathbf{R}-\mathbf{r}_1|}-\frac{1}{|\mathbf{R}+\mathbf{r}_2|}+\frac{1}{|\mathbf{R}-\mathbf{r}_1+\mathbf{r}_2|}\right], \tag{3.6}$$

where $\mathbf{R}$ is the distance between the nuclei with nucleus 1 located at the origin, q is the charge, $\mathbf{r}_1$ and $\mathbf{r}_2$ are the electron displacements of two Drude oscillators, with the corresponding fluctuating dipoles given as $\mathbf{p_1}=q\mathbf{r}_1$ and $\mathbf{p_2}=q\mathbf{r}_2$, and the polarizability is given as $\alpha=q^2/(m\omega^2)$. In this subsection, α denotes polarizability and C denotes the Gaussian width in the OQA.

Under the MSA approximation, each Drude oscillator moves in the potential of mean force due to the other induced dipoles, resulting in a larger amplitude, or equivalently a larger polarizability. For a homogeneous polarizable fluid, the fact that all the Drude oscillators are identical leads to the self-consistency of the renormalized polarizability. Under the MSA assumption the optimized reference oscillator for an isotropic fluid is centered at $\mathbf{r}_1=0$ and $\mathbf{r}_2=0$ so $h_i=0$. Assuming a renormalized polarizability $\bar{\alpha}$, the effective Gaussian width is given by

$$C=\frac{1}{m\bar{\omega}^2\beta}\,\frac{b/2}{\tanh(b/2)}, \tag{3.7}$$

where $b=\hbar\bar{\omega}\beta$ and $\bar{\omega}$ is related to $\bar{\alpha}$ through the expression $\bar{\alpha}=q^2/(m\bar{\omega}^2)$. Then, the Gaussian averaged Coulomb potential is explicitly given as

$$\bar{V}(\mathbf{R},C)=\int d\mathbf{r}\;\rho(\mathbf{r},C)\,\frac{q^2}{|\mathbf{R}-\mathbf{r}|}=\int_R^\infty d\mathbf{r}\;\frac{qQ(r,C)}{r^2}, \tag{3.8}$$

where ρ is the Gaussian distribution function

$$\rho(\mathbf{r},C)=\frac{1}{\sqrt{2\pi C}}\exp(-r^2/2C) \tag{3.9}$$

and $Q(r,C)=\int_0^r\rho(\mathbf{r}',C)d\mathbf{r}'$ is the charge enclosed by a sphere of radius r. Next, the OQA equations Eqs. (3.3) and (3.4) can be approximated in the MSA by the solutions

$$s_i(\mathbf{R},C)\simeq m\omega^2+\partial_i^2\bar{V}(\mathbf{R},C)-\partial_i^2(\mathbf{R},2C) \tag{3.10}$$

and

$$t_{ij}(\mathbf{R},C)\simeq 2\partial_i\partial_j\bar{V}(\mathbf{R},2C)-\partial_i\partial_j\bar{V}(\mathbf{R},C), \tag{3.11}$$

where the partial derivatives are now applied to the three components of $\mathbf{R}$ for any given pair of Drude oscillators [cf. Eq. (3.6)].

Now, one can modify the MSA equation for the optimized polarizable fluids. Among many approaches available, we adopt the matrix formulation developed for nonpolar polarizable fluids, (e.g., Appendix A of the Ref. 19). The renormalization equation for $\bar{\alpha}$ and, in turn, $\bar{\omega}$ is given in this approach by

$$\bar{\alpha}=\frac{\alpha}{1+(\alpha/\bar{\alpha})\Sigma(\bar{\alpha})} \tag{3.12}$$

where Σ can be approximated by Eq. (A6) of Ref. 19 with the dipole–dipole interaction tensor $\mathsf{T}(\mathbf{R})$ replaced by the tensor $\mathbf{t}(\mathbf{R},C)$ from Eq. (3.11), i.e.,

$$\Sigma(\bar{\alpha})=\frac{t_2}{1-(t_3/t_2)}, \tag{3.13}$$

where

$$t_2=\frac{1}{3}\,\bar{\alpha}^2\rho\int d\mathbf{R}\;g(\mathbf{R})\mathrm{Tr}(\mathbf{t}^2) \tag{3.14}$$

and

$$t_3=\frac{\bar{\alpha}^3\rho^2}{3V}\int d\mathbf{R}_1\int d\mathbf{R}_2\int d\mathbf{R}_3\mathrm{Tr}[\mathbf{t}(\mathbf{R}_1-\mathbf{R}_2)\mathbf{t}(\mathbf{R}_2-\mathbf{R}_3)\times\mathbf{t}(\mathbf{R}_3-\mathbf{R}_1)]g_3(\mathbf{R}_1,\mathbf{R}_2,\mathbf{R}_3). \tag{3.15}$$

Here, ρ is the density, V is the volume, and $g_3(\mathbf{R}_1,\mathbf{R}_2,\mathbf{R}_3)$ is the three-body equilibrium distribution function for the fluid. By solving Eqs. (3.11) and (3.12) simultaneously, an optimized self-consistent MSA solution is obtained for the fluid consisting of Drude oscillators. Once the renormalized polarizability is obtained, many properties of the Drude fluid can be approximated at the level of MSA theory by a dipolar fluid with the equivalent dipole moment $|\mathbf{P}|^2=3(\bar{\alpha}/\beta)$.[15–17]

If the dipole–dipole approximation is assumed to dominate the interactions, the different Fourier path modes are decoupled so that the dielectric constant and dielectric response are the same for a classical and a quantum nonpolar polarizable system. However, with the help of OQA theory, one concludes that the nonlinear interaction has a larger effect for quantum systems than for classical systems—and this nonlinear effect increases as the mass and the temperature decrease. In addition, the OQA will provide a vehicle to study *many-body* polarization effects beyond the dipole–dipole approximation.

C. Ground state energy of a perturbed Drude oscillator

As has been demonstrated in Sec. II C, the quantum ground state energy can be obtained from the asymptotic expression of the partition function in the low temperature quantum mechanical limit. It has been shown for the one dimensional case that the OQA equation including higher order corrections is equivalent to solving the Schrödinger equation in a LHO basis set with the help of perturbation theory. The method is below applied to the problem of a highly quantum mechanical Drude oscillator of mass m, frequency ω, and charge q, such that $\{\omega=0.534,\ m=0.245,\ q=1.38\}$ (which are the parameters of, e.g., Xe[44]). This oscillator is perturbed by a Coulomb interaction with an electron fixed in the space. The goal here is to calculate the quantum ground state energy shift of the oscillator, ΔE, due to the interaction with the electron. The positive charge of the Drude oscillator is placed at the origin (0,0,0), while the negative charge oscillates under the linear harmonic potential. The electron is placed at distance R on the x axis at $(R,0,0)$. The potential is thus given by

$$V(\mathbf{r})=\frac{1}{2}\,m\omega^2\mathbf{r}^2-eq\left[\frac{1}{R}-\frac{1}{|\mathbf{R}-\mathbf{r}|}\right], \tag{3.16}$$

where $\mathbf{r}$ is the displacement of the negative charge of the Drude oscillator. At room temperature ($T=300$ K), such that $b=\beta\hbar\omega=545$, the oscillator is dominated by the ground state so that the ground state energy shift is effectively the same as the ''solvation'' energy.

Under the condition that the separation R is relatively large, satisfying $R^2>(\hbar/2m\omega)$, the dipole approximation is valid, implying

$$V_d(\mathbf{r})\simeq\frac{1}{2}\,m\omega^2\mathbf{r}^2-\frac{eq}{r^3}\,\mathbf{r}\cdot\mathbf{R}. \tag{3.17}$$

As a result, the charge–dipole interaction leads to a ground state energy shift of

$$\Delta E_d=-\alpha e^2/2R^4, \tag{3.18}$$

where the polarizability α is explicitly given by $\alpha=q^2/(m\omega^2)$. At smaller separations, the ground energy shift ΔE will be reduced because of the full Coulomb interaction. This reduction is denoted here by the energy correction function $c(R)$ defined as

$$c(R)=\Delta E/\Delta E_d. \tag{3.19}$$

For the sake of comparison with the analytic theory, path integral Monte Carlo simulations have also been carried out to calculate the exact ground state energy shift. Path integral simulations are usually used to study temperature-dependent properties and are generally not efficient for calculating ground state energies. Nevertheless, it was found that the normal mode path integral Monte Carlo method[20] (NMPIMC) is at least as effective as the diffusion Monte Carlo method (DMC) for calculating the ground state energy for the potential in Eq. (3.16). The calculation of the ground state energy shift caused by a small perturbation requires the simulation of a system with a large number of quasiparticles and very long runs because an accurate determination of the difference between two large expectation values is required. One way to circumvent this difficulty is to use the residue potential, $\Delta V=V-V_{\rm ref}$, as a Monte Carlo weighting function instead of a Metropolis importance sampling function. The potential $V_{\rm ref}$ is an arbitrary quadratic reference potential which was chosen to be the OQA potential [Eq. (2.29)] for optimal convergence. This procedure gives

$$\Delta Z(\beta,P)=\langle e^{-(\beta/p)\Sigma_j\Delta V(x_j)}\rangle_{\rm ref}, \tag{3.20}$$

where the average is taken over the configurations generated by $e^{S_{\rm ref}/\hbar}$. In the limit of low temperature, ΔZ yields the ground energy shift due to ΔV, i.e.,

$$\Delta E=-\lim_{\beta\to\infty}\lim_{P\to\infty}\ln\Delta Z(\beta,P). \tag{3.21}$$

For the potential in Eq. (3.16) with $b\geqslant 5$ and $P\geqslant 2^6$, the difference between the exact ground state energy and the average energy is less than 10^{-8}. The NMPIMC simulations were performed at $b=5$ and $P=64$. A total of 10^6 independent configurations were sampled. More details regarding NMPIMC can be found in the relevant papers.[20,45]

In Fig. 3, the function $c(R)$, as obtained from the OQA solution and from the higher order corrections, is plotted from $R=0.5$ to $R=10.0$ along with the exact results obtained from the NMPIMC simulation. The OQA equations and the higher order corrections in the three-dimensional space of $\mathbf{r}$ are given in Sec. II E. The considerable accuracy in the analytical prediction supports the validity of the theory. It must be pointed out that the OQA theory contains more information than just the ground state energy of physical systems: It is essentially the most general possible effective harmonic theory for describing equilibrium systems at a given temperature.

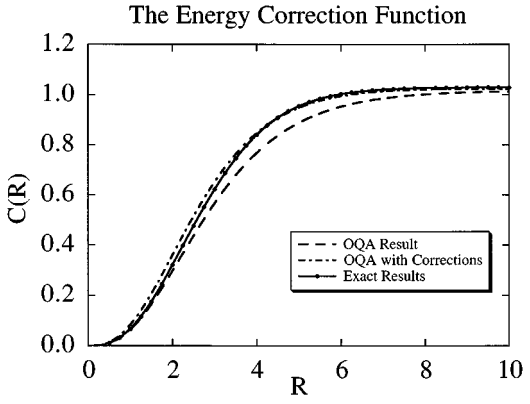

FIG. 3. A plot of the energy correction function $c(R)$ defined by Eq. (3.9). The solid circles are the numerically exact results, while the dashed line is the OQA result from Eqs. (2.27)–(2.28), and the dash–dot line is the result obtained by including the higher order correction from Eq. (2.35).

D. Intramolecular vibrational relaxation in polyatomic molecules

An isolated polyatomic molecule can exhibit a characteristic change in its nonlinear vibrational motion as its en-

ergy increases (see, e.g., Ref. 46). The transition of normal-mode vibrations to stochastic behavior and the rate of intramolecular vibrational relaxation (IVR) can be studied via the techniques of quantum Green's function.[47–49] According to the inverse Wick rotation, the analytical continuation of Euclidean correlation functions gives real time correlation function.[36,37] In fact, the analytical continuation in Fourier space directly yields the Fourier transformation of the quantum response function, namely, the retarded Green's function. Therefore, in studying the breakdown of normal mode behavior in molecules the higher order corrections to the Euclidean correlation function presented in Sec. II D assume an important role in the analysis.

Consider a system described by the Hamiltonian

$$H=\sum_{i=1}^{N}\left(\frac{p_i^2}{2}+\omega_i^2\,\frac{q_i^2}{2}\right)+\frac{1}{3!}\sum_{i,j,k=1}^{N}c_{ijk}q_iq_jq_k, \tag{3.22}$$

where the mass is assumed to be unity, ω_i is the frequency of ith normal mode, and c_{ijk} is the cubic coupling constant. If the normal modes are taken to be the quadratic reference system, one has

$$\bar{q}_{r,i}=0 \tag{3.23}$$

and

$$\alpha_{n,ij}=\frac{1}{\beta(\Omega_n^2+\omega_i^2)}\,\delta_{ij}, \tag{3.24}$$

where Ω_n is the Matsubara frequency defined earlier as $\Omega_n=2\pi n/\hbar\beta$. Since ΔV is the cubic term in Eq. (3.22), the only nonvanishing vertex in the diagrammatic expression is the one linked to three lines, i.e.,

$$\partial_i\Delta V=0, \tag{3.25}$$

$$\partial_i\partial_j\Delta V=0, \tag{3.26}$$

$$\partial_i\partial_j\partial_k\Delta V=c_{ijk}. \tag{3.27}$$

Because of the cubic anharmonicity, the equilibrium position $\bar{q}_i$ is shifted according to Eq. (2.25), giving

$$\bar{q}_i=-\beta\alpha_{0,ii}\sum_{j,k=1}^{N}[c_{ijk}\bar{q}_j\bar{q}_k+\tfrac{1}{2}c_{ijj}\bar{\alpha}_{jj}(0)], \tag{3.28}$$

where it is assumed that the renormalized correlation function matrix is also diagonalized and where $\bar{\alpha}_{jj}(0)=\Sigma_n\bar{\alpha}_{n,jj}$. Next, the infinite summation of two-line-loop diagrams is carried out to yield Eq. (2.48), which can be explicitly written in the present case as

$$\bar{\alpha}_{n,ii}=\alpha_{n,ii}-\beta\alpha_{n,ii}\bar{\alpha}_{n,ii}\sum_{j=1}^{N}c_{iij}\bar{q}_j+\frac{1}{2}\beta^2\alpha_{n,ii}\bar{\alpha}_{n,ii}\sum_{j,k=1}^{N}c_{ijk}^2\sum_{m}\bar{\alpha}_{m,kk}\bar{\alpha}_{n-m,jj}, \tag{3.29}$$

where the convolution results from the two-line loops.

Equations (3.28) and (3.29) represent the self-consistent equations resulting from the renormalization of the dashed and solid lines, and they can be solved iteratively. However, the analytical continuation requires a closed form expression which can be obtained by a perturbation approximation. The final solution takes the simple form

$$\bar{\alpha}_{n,ii}=\frac{\alpha_{n,ii}}{1-\Sigma_{n,ii}}, \tag{3.30}$$

where the leading order in the self-energy term is given by

$$\Sigma_{n,ii}=\frac{\beta^2}{2}\sum_{j,k=1}^{N}\left(c_{iij}c_{jkk}\bar{\alpha}_{kk}(0)\alpha_{0,jj}+c_{ijk}^2\sum_{m}\bar{\alpha}_{m,kk}\bar{\alpha}_{n-m,jj}\right). \tag{3.31}$$

In Eq. (3.31), the first term gives the frequency shift due to the change in the equilibrium positions and the second term give arise to both a frequency shift and the spectral broadening. Essentially, the broadening of the normal mode spectrum is related to the vibrational relaxation.[46] Equation (3.31) is exactly the same as the one derived by Stuchebrukhov *et al.*[21] in their study of threshold energy dependence of intramolecular relaxation in polyatomic molecules. Evidently, their result is a special realization of the general theory in Sec. II as applied to the Hamiltonian in Eq. (3.22).

IV. CONCLUDING REMARKS

In this paper, the representation of physical systems by effective harmonic oscillators has been explored. The resulting optimized quadratic approximation (OQA) has been developed in the general context of statistical mechanics (i.e., systems characterized by a temperature). Mathematically, the formulation is based on a diagrammatic representation of the cumulant expansion for the partition function in terms of multidimensional Gaussian variables. In essence, both classical and quantum statistical mechanics has been recast in terms of a harmonic "basis set." Apart from its possible physical applications, such a formal development is instructive and meaningful in itself.

Through representative physical applications have been discussed in Sec III, the most important application of the OQA theory will be to real continuous media such as solids, liquids, and glasses. The multiple OQA solutions in the many-body hyperspace characterize the nature of the different phases in an "understandable" way and may thereby allow one to better isolate the physical features which lead to the transitions between those phases. As another application, consider the case of liquid state dynamics which may, for transient periods of time, be described by solid state concepts such as "inherent structures"[24–26] or "instantaneous normal modes" (i.e., phonons).[28,29] The present theory can self-consistently describe transient liquid state structures and their thermal fluctuations, while effectively taking into account the anharmonicity of the many-body potential surface as it influences such structures. This approach thereby pro-

vides a well-defined mathematical framework for the intuitive liquid state inherent structure idea introduced by Stillinger and Weber.[24–26]

Aside from calculating statistical properties, another motivation of the present research is to provide a basis for constructing dynamical theories. In fact, in a forthcoming paper[34] the OQA solutions will be used to develop a theory for dynamical time correlation functions in liquids. This theory differs from one based on the concept of instantaneous normal modes,[28,29] providing a sort of ''dynamical inherent structure'' perspective for liquid state dynamics. Given that so much is known about the statistical and dynamical behavior of harmonic systems, it seems likely that the present work will also lead to other interesting and useful effective harmonic models of realistic physical systems.

ACKNOWLEDGMENTS

This research was supported by a National Science Foundation Presidential Young Investigator Award (CHE-9158079) and by a David and Lucile Packard Fellowship in Science and Engineering.

[1] R. P. Feynman, *Statistical Mechanics* (Addison-Wesley, MA, 1972), Chap. 3.
[2] J. Cao and G. A. Voth, J. Chem. Phys. **100**, 5093 (1994).
[3] R. P. Feynman and A. R. Hibbs, *Quantum Mechanics and Path Integrals* (McGraw-Hill, New York, 1965).
[4] L. S. Schulman, *Techniques and Applications of Path Integration* (Wiley, New York, 1986).
[5] M. S. Swanson, *Path Integrals and Quantum Processes* (Academic, San Diego, 1992).
[6] B. J. Berne and D. Thirumalai, Annu. Rev. Phys. Chem. **37**, 401 (1986).
[7] J. D. Doll, D. L. Freeman, and T. L. Beck, Adv. Chem. Phys. **78**, 61 (1990).
[8] D. Chandler, in *Liquides, Cristallisation et Transition Vitreuse Les Houches, Session LI*, edited by D. Levesque, J. Hansen, and J. Zinn-Justin (Elsevier, New York, 1991).
[9] For reviews of numerical and analytical path integral methods, see Refs. 6–8.
[10] See Ref. 3, pp. 303–307, and Ref. 1, pp. 86–96.
[11] R. P. Feynman and H. Kleinert, Phys. Rev. A. **34**, 5080 (1986).
[12] R. Giachetti and V. Tognetti, Phys. Rev. Lett. **55**, 912 (1985).
[13] J. Cao and B. J. Berne, J. Chem. Phys. **92**, 7531 (1990).
[14] H. Kleinert and H. Meyer, Phys. Lett. A 319 (1994). This work is closely related to the diagrammatic formulation of the centroid density in Ref. 2. However, in the latter paper the locally optimized quadratic reference potential approximation was explicitly derived from the perspective of the diagrammatic analysis, thus enabling the introduction of the higher-order corrections without having to subtract the overcounted diagrams resulting from the quadratic optimization. Moreover, it was shown how the lines (i.e., the centroid-constrained imaginary time propagators) could be renormalized along with the vertices in a consistent fashion to substantially improve upon the accuracy of the effective quadratic variational method.
[15] J. Hoye and G. Stell, J. Chem. Phys. **73**, 461 (1980).
[16] L. R. Pratt, Mol. Phys. **40**, 347 (1980).
[17] M. J. Thompson, K. S. Schweizer, and D. Chandler, J. Chem. Phys. **76**, 1128 (1982).
[18] Z. Chen and R. Stratt, J. Chem. Phys. **95**, 2669 (1991).
[19] J. Cao and B. J. Berne, J. Chem. Phys. **99**, 6998 (1993).
[20] J. Cao and B. J. Berne, J. Chem. Phys. **99**, 2902 (1993).
[21] A. A. Stuchebrukhov, M. V. Kuzmin, V. N. Bagratashvili, and V. S. Letokhov, Chem. Phys. **107**, 429 (1986).
[22] T. Morita and K. Hiroike, Prog. Theor. Phys. **25**, 537 (1961).
[23] R. D. Mattuck, *A Guide to Feynman Diagrams in the Many-Body Problem* (McGraw-Hill, New York, 1976).
[24] F. H. Stillinger and T. A. Weber, Phys. Rev. A **25**, 978 (1982).
[25] F. H. Stillinger and T. A. Weber, J. Chem. Phys. **80**, 4434 (1984).
[26] F. H. Stillinger and T. A. Weber, J. Chem. Phys. **81**, 5089 (1984).
[27] R. Zwanzig, J. Chem. Phys. **79**, 4507 (1983).
[28] G. Seeley and T. Keyes, J. Chem. Phys. **91**, 5581 (1989).
[29] B. Xu and R. M. Stratt, J. Chem. Phys. **92**, 1923 (1990).
[30] M. Buchner, B. M. Ladanyi, and R. M. Stratt, J. Chem. Phys. **97**, 8522 (1992).
[31] J. Cao and G. A. Voth, J. Chem. Phys. **101**, 6184 (1994).
[32] M. Born and K. Huang, *Dynamical Theory of Crystal Lattices* (Clarendon, Oxford, 1955).
[33] C. Kittel, *Quantum Theory of Solids* (Wiley, New York, 1963).
[34] J. Cao and G. A. Voth (unpublished).
[35] P. M. Stevenson, Phys. Rev. D **30**, 1712 (1984).
[36] G. Baym and N. D. Mermin, J. Math. Phys. **2**, 232 (1961).
[37] D. Thirumalai and B. J. Berne, J. Chem. Phys. **79**, 5029 (1983).
[38] J. A. Barker and M. L. Klein, Phys. Rev. B7 **73**, 461 (1973).
[39] J. P. Hansen and I. M. McDonald, *Theory of Simple Liquids* (Academic, New York, 1986).
[40] D. E. Logan, Mol. Phys. **51**, 1365 (1984).
[41] J. Cao and B. J. Berne, J. Chem. Phys. **97**, 8628 (1992).
[42] B. Cichocki, B. U. Felderhof, and K. Kinsen, Phys. Rev. A **39**, 5350 (1989).
[43] Y. Chen, J. L. Lebowitz, and P. Nielaba, J. Chem. Phys. **91**, 340 (1989).
[44] M. New and B. J. Berne (unpublished results).
[45] J. Cao and G. A. Voth, J. Chem. Phys. **101**, 6168 (1994).
[46] J. Jortner and B. Pullman, *Intramolecular Dynamics* (Reidel, Boston, 1982).
[47] J. M. Ziman, *Models of Disorder* (Cambridge University, Cambridge, 1979).
[48] E. N. Economou, *Green's Function in Quantum Mechanics* (Springer, Berlin, 1983).
[49] R. Kubo, N. Toda, and N. Hashitsume, *Statistical Physics II* (Springer, Berlin, 1985).